
Article:
Al-Zubidi, M., Widziolek, M., Court, E.K. et al. (10 more authors) (2019) Identification of novel bacteriophages with therapeutic potential targeting Enterococcus faecalis. Infection and Immunity, 87 (11). e00512-e00519. ISSN 0019-9567

https://doi.org/10.1128/iai.00512-19

Identification of novel bacteriophages with therapeutic potential targeting *Enterococcus faecalis*

Al-Zubidi, M[1], Widziolek, M[1,3], Court, E.K.[1], Gains, A.F.[1], Smith, R.E.[2], Ansbro, K[1], Alrafaie, A[1], Evans, C[4], Murdoch, C[1], Mesnage, S[2], Douglas, C.W.I[1], Rawlinson, A.[1] & Stafford, G.P[1]*

Affiliations:

1- Integrated BioSciences, School of Clinical Dentistry,University of Sheffield, 19 Claremont Crescent, Sheffield, S10 2TA, UK
2- Department of Molecular Biology and Biotechnology, University of Sheffield, Firth Court, Western Bank, Sheffield, S10 2TN, UK
3- Department of Microbiology, Faculty of Biochemistry, Biophysics and Biotechnology, Jagiellonian University, Kraków, Poland.
4- Department of Chemical and Biological Engineering, The University of Sheffield, Mappin Street, Sheffield S1 3JD, UK

Corresponding author: Dr Graham Stafford, Integrated BioSciences, School of Clinical Dentistry, University of Sheffield, 19 Claremont Crescent, Sheffield, S10 2TA, UK

Email: g.stafford@sheffield.ac.uk

Tel: +44 114 2254913

Abstract

The Gram-positive opportunistic pathogen *Enterococcus faecalis* is frequently responsible for nosocomial infections in humans and represents one of the most common bacteria isolated from recalcitrant endodontic (root canal) infections. *E. faecalis* is intrinsically resistant to several antibiotics routinely used in clinical settings (such as cephalosporins and aminoglycosides) and can acquire resistance to vancomycin (vancomycin resistant enterococci, VRE). The resistance of *E. faecalis* to several classes of antibiotics and its capacity to form biofilms cause serious therapeutic problems. In this paper, we report the isolation of several bacteriophages that target *E. faecalis* strains isolated from the oral cavity of patients suffering root-canal infections. All phages isolated were *Siphoviridae* with similar tail lengths (200-250 nm) and icosahedral heads. The genome sequences of three isolated phages were highly conserved with the exception of predicted tail protein genes that diverge in sequence, potentially reflecting host range. The properties of the phage with the broadest host-range (SHEF2), was further characterised. We showed that this phage requires interaction with components of the major and variant region Enterococcal polysaccharide antigen (Epa) to engage in lytic infection. Finally, we explored the therapeutic potential of this phage and showed that it can eradicate *E. faecalis* biofilms formed *in vitro* on a standard polystyrene surface but also on a cross-sectional tooth-slice model of endodontic infection. We also show that SHEF2 cleared a lethal infection of zebrafish when applied in the circulation. We therefore propose that the phage described in this study could be used to treat a broad range of antibiotic resistant *E. faecalis* infections.

Introduction

Enterococcus faecalis is a common nosocomial pathogen that is a frequently isolated from the blood stream and wound infections (1, 2). In some cases, the clinical outcomes are poor due to the limited choices of effective antimicrobial therapy and colonisation by vancomycin-resistant enterococci (VRE). One example is *E. faecalis* strain V583, which was the first of the vancomycin-resistant *E. faecalis* clinical isolates to be sequenced (3, 4). In addition *E. faecalis* is commonly recovered from chronic periapical or root canal infections associated with failed endodontic therapy (5, 6). It has been proposed that this is associated with their ability to (i) live and survive in the presence of several commonly used root canal antiseptic irrigants (e.g., calcium hydroxide) (7), (ii) tolerate prolonged periods of starvation (8), (iii) form biofilms (9) and (iv) acquire antibiotic resistance (10, 11) –together this indicates that new therapeutic approaches are necessary.

Bacteriophage therapy has recently re-emerged as an attractive alternative antimicrobial strategy to treat antibiotic resistant biofilm forming pathogens. In some infections such as those associated with burn wounds caused by *Pseudomonas aeruginosa* and *Staphylococcus aureus*, phage therapy is now considered an option for topical application (12). Furthermore, in the United States, the FDA recently approved a phage-based phase I clinical trial against *P. aeruginosa. Staphylococcus* and *Esherichia coli* in chronic venous leg ulcers, illustrating that treatment using a phage cocktail was associated with no adverse reaction (13). For example, phase II clinical trials in Europe using phage therapy against chronic otitis externa caused by *P. aeruginosa* infection have been conducted with successful results (14). Excitingly, phage were also used intravenously in 2019 to cure a disseminated *Mycobacterium abscessus* infection in a 15-year old in the UK (15)

E. faecalis lytic phages have been previously isolated using indicator strains of animal origin (16, 17), non-oral human isolates and lab strains (18-21). Here, we set out to isolate

bacteriophages targeting *E. faecalis* strains of oral origin, isolated either directly from endodontic infections or from mouthwashes of patients receiving endodontic treatment, and from oral lesions sourced from a range of oral microbiology laboratories around Europe. A range of tailed phages were isolated from a wastewater treatment plant and characterized. We report their therapeutic potential against *E. faecalis* strains forming biofilms and their capacity to eradicate systemic infection in a zebrafish model of infection. Overall our data further highlight that phages have great potential as therapeutic adjuncts in oral and other infections.

Materials and methods

Bacterial Strains used for bacteriophage screening. Bacterial strains used in these investigations and their sources are listed in Table 1 (22). *Enterococcus* strains were grown aerobically with 5% CO_2 at 37°C on brain heart infusion (BHI) agar (OXOID, UK).

Bacteriophage isolation. Bacteriophages were isolated from wastewater collected from the inlet of a water treatment plant in the Sheffield area (UK) that treats both industrial and domestic wastewater. The water was filtered through 3M filter paper on-site to remove particles but was not treated chemically or biologically. Samples were immediately brought to the laboratory and centrifuged 7,000 *x g* for 15 min to remove remaining debris. The resulting supernatant was then passed through a 0.45 µm filter (Sartorius, Germany) before 200 ml of sample were further centrifuged at 35,000 *x g* for 90 min to pellet any phage particles. The pellets were carefully resuspended overnight in 2 ml of SM buffer (1 M Tris-HCl Buffer pH 7.4 with 5 M NaCl, 1 M $MgSO_4$ and 1% Gelatin) at 4°C. 10 µl of the suspended sample was spotted on to a double layer agar plate. The bottom agar was composed of BHI solid agar supplemented with 5% (v/v) horse serum (OXOID, UK) and was overlaid with 3-4 ml of molten BHI soft agar (0.7%) containing 200 µl of test bacterial strain (overnight culture inoculum, OD_{600} ~ 2). Any formed plaques were picked using a sterile Pasteur pipette, deposited in 1 ml SM buffer and incubated

overnight at 4°C before filtering through a 0.45 µm syringe filter. Isolated phage were then expanded by infection using 100 µl of this with 200 µl of exponential growth phase indicator bacteria for 10 minutes before mixing with 2-3 ml soft agar overlay (SAO) and overnight incubation at 37°C. All phage were purified using three consecutive rounds from single-plaques. The plaques from the third round were then re-suspended in SM buffer containing 0.1% (v/v) chloroform and stored at 4°C.

Phage stock preparations. In order to prepare a working phage stock with known plaque forming unit numbers (PFU), 40 ml exponential growth indicator bacteria was infected with 100 µl of stored phage suspension, incubated for three hours at 37°C to allow phage to multiply and increase in number. The broth was then centrifuged at 7,000 xg for 15 min and passed through a 0.45 µm filter. Serial dilutions from the resultant broth was used in triplicate for plating in over-layer SAO as previously described and PFU/ml for each isolated phage calculated.

Transmission electron microscopy. Purified phage particles in SM buffer were placed onto carbon-coated copper grids and negatively stained with 2% (wt/vol) uranyl acetate for 1 min. Particles were visualised using a FEI Tecnai G2 Spirit Transmission Electron Microscope at an accelerating voltage of 80kV at the Electron Microscopy Unit in Sheffield. Electron micrographs were recorded using a Gatan Orius 1000 digital camera and Digital Micrograph software. To observe the phage along with bacteria, 1 ml exponentially growing cells were infected with phage at multiplicity of infection (MOI) of 1 for 30 min, after centrifugation at 7000 xg for 10 min, the pellet was re-suspended with 1 ml 3% glutaraldehyde for one hour (room temperature) and examined by TEM as described above.

Bacteriophage concentration by precipitation with Polyethylene Glycol (PEG 8000). Further concentrations of phage was made in order to yield a suitable working suspension for protein profiling, genomic digestion, and DNA extraction. This was performed by precipitation

with PEG 8000 (23). Briefly, 200 ml of exponential phase indicator bacteria were infected with phage stock at MOI 0.01 for three hours before 1 M NaCl was added during continuous mixing at 4°C for one hour before any unlysed bacteria and cell debris were removed by centrifugation (5000 xg). To precipitate phage particles, 10% PEG 8000 w/v was gradually added with continuous mixing and left overnight at 4°C before centrifugation at 11,000 xg for 20 min to sediment precipitated phage. The resulting pellets were carefully re-suspended overnight with 1 ml of SM buffer and stored at 4°C.

Heat-inactivation of phage. A phage suspension at $1x10^{11}$ PFU/ml was treated for 45 mins at 80°C- which we established inactivated the virus with a 7-log -fold drop in PFU/ml.

One-step growth. We used the procedure described by (24) with some modifications. Briefly, 5 ml of exponentially growing cultures of *E. faecali*s OS16 were infected with SHEF2 phage at MOI of 0.1. After 5 min of phage adsorption, bacteria were diluted 200 times (to prevent further infection), and incubated at 37°C. Two samples were taken every 5 min with one used to enumerate free-phages in solution; the second was treated with 1% (v/v) chloroform to release intracellular phage and was used to enumerate total phage number. Phage titers were determined as described previously and plaques counted on double layer agar plates.

Analysis of phage proteins. To define the major proteins present in the bacteriophage SHEF2, 4, 5, 6, and 7, SDS-polyacrylamide gel electrophoresis (PAGE) was performed. A PEG 8000 concentrated phage stock was mixed with an equal volume of chloroform in order to release the phage particles before vortexing until an emulsion formed and centrifuged at 10,000 xg for 10 min. 50 µl from the upper layer (10^{11}-10^{13} PFU/ml) was then mixed with 50 µl of SDS-PAGE loading buffer and heated at 95°C for 7 min. 10 µl of lysate was loaded directly onto 4-12% NuPAGE® Bis-Tris precast gels (Thermo fisher scientific, UK) and electrophoresed for 60

min. Gels were stained with InstantBlue (Expaedeon) and imaged using a gel documentation system (Image scanner power look1120 USG, Amersham Bioscience).

Mass spectrometry

In gel digestion. Gel bands were excised and diced into 1 mm pieces prior to destaining using 200 mM ammonium bicarbonate (NH_4HCO_3), 40% v/v acetonitrile (ACN). Samples were reduced and alkylated by sequential addition of 10 mM dithiothreitol, 50 mM NH_4HCO_3, 50°C for 30 min and 55 mM iodoacetamide, 20 min at room temperature in the dark. Gel pieces were dried using ACN, before rehydration into a 10 ng/µl solution of trypsin prepared in 50 mM NH_4HCO_3. Samples were digested overnight at 37°C. Peptides in the supernatant were harvested, and combined with peptides obtained by extraction of the gel pieces using 97% ACN, 0.1% (v/v) Formic acid (FA). Peptides were dried by centrifugal evaporation using a Scanvac vacuum centrifuge (Labogene, Denmark) connected to a Vacuubrand Vacuum Pump (Vacuubrand, Germany) before resuspension in 3% v/v ACN, 0.1% trifluoroacetic acid (TFA).

LC-MS/MS. Peptides were analyzed by nano-HPLC (UltiMate 3000 HPLC System, Thermo, Hemel Hempstead, UK) coupled to an amaZon ETD MS ion trap spectrometer (Bruker Daltonics, Bremen, Germany) using nano-ESI spray. The nano-HPLC system and the ion trap spectrometer were controlled using the Bruker Compass HyStar v3.2-SR2 software. The liquid chromatography system comprised a reversed-phase precolumn (LC Packings, Dionex) for sample desalting and PepMap 100 reversed-phase C18 column, 75 µm x 15 cm (Thermo, Hemel Hempstead, UK), for peptide fractionation. The flow rate for precolumn loading was 30 µL/min of loading buffer (97% v/v ACN, 0.1% (v/v) TFA). Peptides were analysed at a flow rate of 300 nL/min and separated by gradient elution using Buffer A (3% v/v ACN, 0.1% (v/v) FA) and Buffer B (97% ACN, 0.1% FA (v/v)): 4% B (0-5 min), 5-38% B (5-65 min), 38-90% B (65-68 min), 90% B (68-73 min), followed by re-equilibration at 4% B. The electrospray was operated in positive ion mode with 4500 V spray voltage and 10 psi gas pressure, 150°C dry gas. The

end plate offset of the mass spectrometer was set to −500 V and for the acquisition the standard method Proteomics Auto MSMS.

Database searching. Protein identifications were obtained using the Mascot software platform (MatrixScience, in house server) to perform database searching against both the EMBOSS 6.5.7.0, and CDS annotation for phage SHEF2 sequence (Accession Number MF678788). Contaminants such as human skin keratin and trypsin were assigned by parallel searching against the cRAP UniProt database (116 sequences, 38,459 residues; downloaded 30 Jan 2015) database. A concatenated target-decoy database search strategy was also employed to estimate the rate of false discovery rate. MS/MS search parameters were Search Enzyme: Trypsin; Max missed cleavages: 1; Fixed modifications: Carbamidomethyl (C); Variable modifications: Oxidation (M); Mass values: Monoisotopic; Protein mass: Unrestricted; Peptide mass tolerance: ± 1.2 Da; Fragment mass tolerance:± 0.6 Da; Instrument type:ESI-TRAP.

MLST designation of strains used. To establish the MLST (multi locus sequence type) profile of each of the strains used, Genomic DNA was extracted using the Wizard Genomic DNA extraction kit (Promega), followed by PCR using the primers previously described (25) The purified PCR fragments were sequenced in both directions by GATC Biotech AG using the same primers. Sequence type (ST) and cluster allelic profiling were determined using the eBURST V3 software accessible via the Internet-accessible data-base (http://efaecalis.mlst.net/;) (26, 27). MLST designations are presented in table 3

Phage DNA extraction. To remove contaminating DNA and RNA from the PEG 8000 concentrated phage stocks, a 10 µg/ml DNase and RNAse solution was added and incubated at 37°C for 30 min before 100 µg/ml of proteinase K was added to degrade nucleases at 50°C for 45 min. Removal of proteins from nucleic acids was achieved by extraction with phenol: chloroform: isoamyl alcohol (25:24:1 v/v). DNA was precipitated by adding two volumes of ice

cold ethanol and incubated overnight at -20°C before DNA was pelleted at 16,000 xg for 20 min, and washed with 70%, before DNA was dissolved in sterile milli-Q-water and stored at -20°C. These samples were used for nucleotide sequencing and restriction fragment length polymor sm (RFLP) analysis of phage genomes.

Restriction fragment length polymor sm (RFLP) and analysis of phage genome size. Phage genomic DNA was subjected to restriction digestion with *Hind*III, *Nde*I and *Mfe*I, (New England, Biolabs, UK) according to manufacturers instruction. The digested products were separated by 1% ETBr-agarose gel electrophoresis to determine RFLP patterns and gels visualised using an Ingenius 3 gel-doc system, (SYNGENE).

Genome sequencing of phages SHEF2, SHEF4 and SHEF5. Pure phage genomic DNA (20 µg) was sequenced by MicrobesNG on an Illumina MiSeq platform with 2 x 250 bp paired-end reads before identification of the closest available reference genome using Kraken (28), and reads mapped using BWA mem (29) to assess the quality of the data. Reads were trimmed using Trimmomatic (30) before *de novo* assembly using SPAdes (31). An automated annotation was performed using Prokka (32), before Mauve align software tool (33) was used to perform visual multiple comparisons while multiple sequence alignment of individual genes was performed using Multalin (34). In addition, PHAST (PHAge Search Tool) (35) and PHASTER (PHAge Search Tool Enhanced Release) (36) web servers were used for further confirmation of annotated phage genomes. Conserved protein domains (where relevant) were detected using Pfam (37). Complete genomes were visualized using Artemis (38) and submitted to the NCBI as individual contigs with accession number MF678788, MF678789 , and MF67878890 for SHEF2, SHEF4, and SHEF5 respectively.

Biofilm assay on polystyrene plates. The ability of the enterococcal strains to form a biofilm on an abiotic surface was quantified based on a previously described method (39). Briefly, *E.*

214 *faecalis* strains were grown overnight in BHI at 37°C. The cultures were diluted 1:40 in fresh BHI
215 medium and 1 ml of this cell suspension was used to inoculate sterile flat-bottomed 48-well
216 polystyrene microtiter plates (Cellstar, Greiner Bio-One). Six wells per strain were inoculated
217 with BHI alone as negative controls. These were then incubated under stationary conditions
218 (aerobic) at 37°C for the time indicated. For longer term biofilms, the media was changed every
219 24 h. Broth was then carefully drawn off from wells and 1 ml fresh broth containing 10^8 PFU/ml
220 SHEF2 phage or BHI only controls were added before incubation for another 3 h. Wells were
221 then gently washed three times with 1 ml of phosphate-buffered saline (PBS). The plates were
222 inverted on a paper towel, air-dried and stained with 1% crystal violet for 15 min. The wells were
223 washed again 3 times, and the crystal violet was solubilized in 500 µl of ethanol-acetone (80:20,
224 v/v) and OD_{570} measured using a microplate reader (Tecan infinite 200, Austria). Each assay
225 was performed in triplicate and repeated three times.

226 **Adsorption rate experiments.** The adsorption rate experiments were performed according to
227 the procedure described previously (40) with small modifications. Briefly, overnight cultures of
228 the bacterial strains were diluted 1:100 in BHI medium. When the OD_{600} of the reference strains
229 reached 2.0, 1 ml of culture was diluted 10-fold in fresh BHI (5 x 10^8 CFU/ml). Phages were
230 added at an MOI of 1 to the diluted culture, mixed gently, and incubated at 37°C. Incubation was
231 continued for 12 min, with samples (100 µl) collected at one-min intervals and diluted
232 immediately in 900 µl cooled SM buffer. The diluted samples were centrifuged at 10000 xg
233 (4°C) for 5 min and passed through a 0.45 µm filter. Finally, the titres of unabsorbed phages in
234 the supernatant were determined after serial dilution. The adsorption levels were represented by
235 the percentage of the total number of phages: calculated as follows: [(initial phage titer / free
236 phage titer in supernatant) /initial phage titer] x 100.

237 ***In vitro* biofilm assay on tooth root surface.** The ability of SHEF2 phage to eradicate *E.*
238 *faecalis* biofilm on extracted natural root surface was quantified based on a previously described

239 method using Resazurin dye change (41, 42). To produce a growth surface, 1 mm thickness
240 root slices were cross sectioned above the root bifurcation area of multi-rooted human teeth
241 (ethical approval number STH18841) by water cooled 0.1 mm cutting saw (MEDREK 859088)
242 and were divided into two groups in 24-well microtitre plates (Cellstar, Greiner Bio-One) with
243 final equal surface area for each group. 7 day (168 h) *E. faecalis* biofilm was grown as
244 described previously - i.e. 24 h media changes. After that, the first group (treated) was treated
245 with 1 ml BHI contain 10^8 PFU/ml SHEF2 phage with BHI only used as a control (untreated)
246 before incubation for another 3 h. The root slices were transferred into 48-well microtitre plates
247 and washed three times with 1 ml PBS. After treatment and washing, 0.350 ml of PBS
248 containing resazurin solution at a final concentration of 1 µg/ml were added to both groups in a
249 48-well plate and incubated at 37°C for 20 min. 0.3 ml from each well of both groups (treated
250 and untreated) was transferred to 96-well microtitre plates and fluorescence was read using a
251 microplate spectrofluorometer (Tecan infinite 200 at λ_{exc} 570 nm, λ_{em} 590 nm). The reading of
252 the non-emitting dye of resazurin (treated) was subtracted from a control group that contained
253 only the resazurin dye. This assay was repeated 2 times with at least 3 samples in each group.
254 In addition we performed a standard curve of bacteria (CFU/ml) vs resazurin (Fig S3C).

255 **Zebrafish as *in vivo* model for phage treatment.** Zebrafish maintenance and experimental
256 work was performed in accordance with UK Home Office regulations and UK Animals (Scientific
257 Procedures) Act 1986. Ethical approval was given by the University of Sheffield Local Ethical
258 Review Panel. Wild-type (WT) inbred zebrafish larvae were obtained from The Bateson Centre,
259 University of Sheffield. All larvae were maintained in E3 medium at 30°C according to standard
260 protocols and monitored for up to 4 days post-fertilization (dpf). Groups of at least 20 larvae
261 were used for each treatment condition. Tricaine-anesthetized embryos were injected
262 individually with 2 nl of *E. faecalis* (30,000 CFU) into the Duct of Cuvier of dechorionated
263 embryos at 30 hours post-fertilization (hpf) and larvae were incubated for 2 h before injection

with 2 nl of SHEF2 phage (MOI of 20, in relation to the original bacterial innoculum) or PBS. Fish health status was monitored for up to 72 hours post-infection (hpi). In parallel larvae were also injected with either PBS only, *E. faecalis* only or Phage only alongside heat-killed phage. In all cases, fish health status was monitored for up to 72 hpi. Zebrafish mortality was assessed based on the examination of the presence of a heart beat and blood circulation (43). Images of 10% formalin-fixed zebrafish larvae were captured using a fluorescence zoom microscope (Axio Zoom.V16, Zeiss) with Zen Black software.

Assessment of phage adhesion. Phage adsorption rates were established as described earlier, with free phage particles of SHEF2 were counted at 0, 10 minutes, and 24 h post-infection with *epaB* mutants cells and compared to control OG1RF cells. The free phage particles was also counted from 24 h suspension after treatment with 1% (v/v) chloroform in order to lyse all cells to release any possible trapped intracellular phage. In addition, 1 ml samples from the 24 h phage-bacterial suspension was pelleted and re-suspended in ice cold 1 ml PBS in 0.28 M NaCl (previously shown to breakdown electrostatic interactions between phage and cell wall material (23) for 10 min at 4°C. These samples were then passed though a 0.45 µm filter to collect phage released, and the titre of free phage in the supernatant established. The phage count from the 0.28 M NaCl sample was deducted from the free phage count of the control group of PBS (0.150 M NaCl) to assess how many were adsorbed and released by increased NaCl. Additionally, and to exclude cell lysis caused by increasing the molarity of NaCl, CFUs were assessed and compared to the control group. This experiment was repeated twice in triplicate each time.

Statistical analysis. Statistical analysis was performed using t-test using Graphpad Prism v7.0 (GraphPad, La Jolla, CA) and statistical significance was assumed if $p<0,05$. For zebrafish experiments, Kaplan-Meier survival curves were compared using log rank test and differences between unhealthy groups were evaluated using One-way ANOVA.

Results

Isolation and characterisation of bacteriophages targeting *E. faecalis*

Sheffield wastewater was used as a potential source for *E. faecalis* specific bacteriophage (several samples from independent sites). Phage plaques were first identified by spotting the processed sewage solution on top-agar lawns of a range of orally isolated clinical strains of *E. faecalis* (Table 1), with plaques successfully obtained with *E. faecalis* OS16, EF2, EF3 and OMGS3919. To isolate individual phages, this procedure was repeated twice and five bacteriophages named SHEF2, 4, 5, 6, 7 were identified using a range of *E. faecalis* isolates (Figure 1)

Three distinct plaque morphologies were identified with SHEF2, 5, 6 and 7 phage forming plaques with 3-4 mm diameter surrounded by a thin area of secondary lysis of 1 mm, while SHEF4 formed 2 mm diameter central plaques surrounded by halos of larger secondary lysis (Figure 1A). When infecting the strain OG1RF, SHEF7 formed small pin hole-sized plaque of 1 mm diameter without distinct secondary lysis while it forms large plaques with OMGS3919 (Figure 1A).

Negative staining transmission electron microscopy of purified phages revealed that all bacteriophages had polyhedral head-shapes and non-contractile long tails ranging from 200 to 250 nm and polyhedral heads (Figure 1B) with diameters between 41-46 nm (Table 2). According to the guidelines of the International Committee on Taxonomy of Viruses (ICTV, 2005), the SHEF bacteriophages were classified as belonging to the family *Siphoviridae* (order *Caudovirales*) based upon their tail morphology (44).

Molecular characterisation of isolated phages

311 Digestion of phage DNA with restriction enzymes and DNase I indicated that all isolated
312 phages were double stranded DNA viruses. Restriction fragment length polymorphism (RFLP)
313 tests were performed on phage chromosomal DNAs (Figure 1C). The restriction profiles of
314 SHEF2 and 6 were very similar, whilst all the others were different. From the RFLP analyses,
315 the five phage genome sizes were estimated to be in the range of 39-43 kbp. Next, we analysed
316 purified phage particles by SDS-PAGE (Figure 1D). Distinct protein profiles suggested five
317 separate phage were isolated. All samples revealed a prominent band at 36 kDA (Figure 1D),
318 which Mass Spectrometry confirmed as the phage major capsid protein for SHEF2 (Figure 2,
319 SHEF2_07). While it is likely that this band is the head protein in all cases, we do not have MS
320 data to confirm this. In short, we successfully confirmed the isolation of five separate *E. faecalis*
321 bacteriophage of the family *Siphoviridae*.

322 **Determination of host-range**

323 The host-range of the phages isolated was studied using both spot and SAO methods at
324 MOI of 0.1 to detect visible plaques. All five SHEF bacteriophages were specific to *E. faecalis*
325 as none were capable of producing visible plaques using *E. faecium* (data not shown). Host-
326 range tests showed that all phage have distinct strain specificity preferences, with SHEF2
327 displaying the broadest host-range with capacity to lyse 9 out of 13 *E. faecalis* indicator strains
328 tested, followed by SHEF6 and 7. SHEF5 and 4 possess the narrowest host-range, lysing only 3
329 and 2 strains, respectively. Despite the similarities between SHEF2 and 6 at the genomic level,
330 their host-range is not identical, indicating they are distinct phage. No relationship between
331 host-range and MLST type was found.

332 **Genome organization of SHEF2, 4 and 5.**

333 The genomes of phages SHEF2, 4 and 5 revealed similar sizes of 41.7, 41.1, and 41.6
334 kbp respectively and appeared to be organised into two halves, transcribed in opposite
335 directions (Figure 2A). Each genome was assembled into one large contig with low read
336 mapping coverage at the 5' and 3' ends and no clear edges at the ends of the contigs,
337 suggesting circularity of terminally redundant permuted genomes. Four gene clusters
338 corresponding to DNA packaging, structural components, cell lysis and, regulation and
339 replication were identified (Figure 2A,B). There is little noncoding DNA between these genes,
340 suggesting single transcripts for each set of genes. Although each phage exhibits a different
341 host range, a high identity was found for both DNA and primary amino acid level of between 77
342 and 94% (see Figure S1). Importantly, no putative integrase encoding genes were detected in
343 the genome sequences, suggesting that the SHEF phages are likely to be lytic in nature.

344 All SHEF phages share a similar distribution pattern for DNA packaging and head
345 morphogenesis genes (Figure 2A, orange), and are upstream of the terminase (45, 46). The
346 predicted head module (Figure 2A, cyan) harbours genes encoding portal proteins (for genome
347 injection into host cells), prohead protease maturation, head capsid proteins and head-tail
348 adaptor proteins. These genes are followed by tail and tape-measure proteins (Figure 4A,
349 green) and a lysis module (Figure 2A, yellow) containing a putative haemolysin XhlA, putative
350 holin and endolysin genes. SHEF2 and 5 encode putative endolysins (SHEF2_21
351 andSHEF5_49) with an N-terminal Amidase_2 domain and a predicted C-terminal
352 ZoocinA_TRD (pfam16775) domain. SHEF4 encodes a putative endolysin with the same N-
353 terminal domain but an SH3b peptidoglycan-binding domain, indicating differing cell-wall
354 targeting mechanisms.

355 The replication and regulation module are also clustered and ordered identically, except
356 that SHEF4 encodes for an adenine-specific methyltransferase (modification methylase *Dpn*IIB)
357 that is absent from SHEF5. In addition, SHEF4 and 5 harboured an additional putative

358 transcriptional regulator gene that is absent from SHEF2 and suggest that all three employ
359 slightly different modes of post-replication and DNA modification that might be key during the
360 infection cycle.

361 Phage tail proteins are involved in the primary recognition and adsorption to specific
362 receptors on the bacterial cell surface (47, 48). Since SHEF2, 4 and 5 exhibit different host
363 ranges, we examined the amino acid sequence of the predicted tail proteins (Figure 2B). The
364 first three proteins displayed a high sequence similarity (81-100%). In contrast, the N-terminal
365 130 aa (out of 695 aa) of the fourth tail protein (SHEF2_16, 4_08 and 5_53), shares very high
366 similarity (>95%) across our phage, while the rest of the sequence was highly divergent (Figure
367 S2A). We obtained similar results with the fifth tail protein (SHEF2_17, 4_09 and 5_52), where
368 the first 175 amino acids (out of 800 aa) encode conserved putative tail domains (TIGR01665
369 and pfam06605), before the rest of the protein sequence diverges (Figure S2B). We propose
370 that these two genes may be key to the host-range determination of these phage during
371 infection as has been seen for other *E. faecalis* phage (51) and represent alternate cell-wall
372 binding proteins and domains.

373

374 **Identification of the enterococcal polysaccharide antigen as the SHEF2 receptor**

375 To gain further insight into the mechanisms driving strain specificity in these phage we
376 sought to identify the receptor for SHEF2. We considered a candidate to be the prominent cell
377 surface rhamnopolysaccharide enterococcal polysaccharide antigen (EPA) (49-51). The genetic
378 locus encoding the synthesis of EPA is composed of 18 highly conserved genes (*epaA-R*)
379 followed by a variable region which is divergent between strains (Figure 3A) (22), and which has
380 been proposed to encode strain specific decoration of the core polysaccharide synthesised by a
381 conserved genetic region (22, 52). Disruption of *epaB* (strain TX5179(*epaB*)), a key rhamnosyl
382 transferase involved in EPA backbone synthesis, abolished infectivity of SHEF2 with infectivity

restored upon complementation with a plasmid containing the *epaBCD* operon (Figure 3B). We then tested infection of strain *oatApgdAdltAsigV*, characterised by Smith et al (22) that has altered Peptidoglycan and Teichoic Acid production, showing that it is still sensitive to infection and that these molecules are not receptors for SHEF2.

As mentioned above, the core EPA is further decorated by variable chemical modifications that modulate virulence. We next tested the infectivity of SHEF2 against mutants in the *epa* variable region using mutants previously shown to impair EPA decorations and virulence (22). Three of the mutants had insertions in genes encoding glycosyl transferases (*OPDV_11720::Tn, OPDV_11715::Tn* and *OPDV_11714::Tn*) and one had an insertion in an epimerase gene (*OPDV_11707::Tn*). All variable region mutants showed a markedly reduced infectivity by SHEF2 which was restored upon *in trans* complementation. Interestingly, the *OG1RF_11714* mutant was still partially infected by SHEF2, with a slightly opaque plaque observed, that was restored to a typical clear plaque by complementation (Figure 3B and S4).

Despite this lack of infection of *epa* mutant strains, it was still possible that binding occurred but that the phage was unable to complete its full lytic cycle. To explore this possibility we carried out an adsorption assay. In this assay, phage and bacteria were incubated together for 24 hours to allow adsorption of phage/ or infection to proceed before the addition of 0.28 M NaCl, a treatment known to interfere with electrostatic phage-bacterial interactions, but not harm *Enteroccocus* cell viability. For strain TX5179(*epaB*) total phage numbers did not increase over 24h- again indicating lack of infection and expansion as compared to the OG1RF strain (Figure 3C). However, the NaCl treatment released $1.4x10^5$ PFU/ml of phage (51.8%, $P<0.01$ vs OG1RF, _11720), reflecting weak adsorption of phage that do not enter a lytic life cycle but are still viable. Adsorption without population increase was also observed with the *OPDV_11720::Tn2.5* however less phage were recovered after 0.28M NaCl treatment (1.75%, $P<0.01$ vs OG1RF, *epaB*) indicating a stronger interaction with more phage left adsorbed after

NaCl treatment. To exclude the possibility that phage progeny were trapped inside the host cells that could not lyse the host membrane and escape, cell suspensions were treated with chloroform, with no further release of viable phage particles. Finally, to examine qualitatively that the released phage is bound to the cells, electron microscopy was performed on OG1RF, TX5179(*epaB*) and *OPDV_11720::Tn2.5* cells cultured with phage. Indeed phage could be observed on all these strains (Fig. 3D) indicating that cell surface binding is still occurring in these mutants and that the core and variable EPA are both bound by phage SHEF2. Like others (51) we observed rounded cell morphology in TX5179(*epaB*) (Fig. 3D), and also with the *OPDV_11720::Tn2.5* strain.

Infection parameters and strain preference of SHEF2

We further characterised the host range and infection characteristics of bacteriophage SHEF2. As shown in Figure S5A strain OS16 (alongside ER3/2s and EF54) was highly sensitive to SHEF2, as assessed by time course infection experiments, with cultures lysing within the first 60 minutes, compared to strains such as OMGS3197, 3919 or 3198 which lyse in mid (2h)- and V583 in late (3h)- exponential phase, respectively (Fig. S5). As a result and since it is an orally isolated clinical strain, we used strain OS16 to perform a one-step growth experiment to establish the eclipse period (average time to produce the first mature intracellular phage), latent period (average time to cell lysis) and burst size (the average number of phage released at cell lysis), which showed SHEF2 as a highly efficient *E. faecalis* targeting phage with an eclipse period of only 10 min, a latent period of only 30 min (Figure 4A), and a burst size of 9.3 PFU for this strain. The plateau phase was reached after 75 min, following a 45 min burst period. Next, we examined adsorption parameters of this phage with the *E. faecalis* strain OS16, and found that saturation of adsorption was reached after 10 min (Figure 4B). This adsorption is illustrated in Figure 4C where a TEM taken of cells at 30 min post infection illustrates attached phage attached to the cell surface.

433

434 **Ability of SHEF2 to clear *E. faecalis* biofilms**

435 Given that most bacteria in nature and in clinical infections reside in biofilms (53, 54) we tested
436 the ability of SHEF2 to eradicate *E. faecalis* biofilms *in vitro* on inert polystyrene surfaces,
437 using a range of strains. As seen in Figure 5A, we tested the phage against 24h preformed
438 biofilms, using heat-killed phage as a negative control, and showed phage-dependent
439 clearance- to varying degrees (3-10-fold), of all sensitive strains (EF54, OS16, OG1RF), while
440 we observed no clearance for strains EF3 and OG1RF-*epaB*, which were insensitive to phage
441 infection in plate based and broth based assays. In addition, we tested clearance of biofilms of
442 strains EF54 and OS16, as well as a mixed strain biofilm that had been preformed for 6-days
443 (FigS3 A,B), again showing clearance of biofilm in a phage dependent manner.

444 We next tested the efficacy of phage SHEF2 to eradicate biofilms on natural tooth root
445 surfaces by growing EF54 biofilms for 168 h before adding SHEF2 ($1x10^8$ PFU/ml) for 3 h, and
446 achieving a significant reduction in bacterial numbers, as indicated by reduction in detectable
447 metabolic activity (Figure 5B, $P<0.0001$) (resazurin assay) to approximately $7x10^3$ bacteria in
448 total estimated using standard curves of Emission ((@590nm) vs CFU/ml Fig. S3C), from an
449 original input of over $1x10^6$ (N.B. we were unable to do this on more strains due to limitations of
450 available tooth slices and ethics restrictions). We also observed, qualitatively, a drastic
451 decrease in bacterial material via reduction in visible bacterial biomass visualised as the dark
452 material in this image using stereomicroscopy and light microscopy (Figure 5C).

453 **Phage treatment evaluation in a zebrafish model of infection**

454 Next, we performed systemic infection studies using an established zebrafish model of
455 infection (55) and the clinical strain OS16. Zebrafish embryos were infected with *E. faecalis* for

456 two hours before injecting with SHEF2 or a heat-killed sample of SHEF2 at a multiplicity of
457 Infection (MOI) of 20 (with respect to the *E. faecalis* inoculum), alongside virus only controls.
458 Fish mortality and health status was then monitored up to 72 hpi. *E. faecalis* OS16 caused a
459 time-dependent lethality that was significantly higher (p<0,0001) than PBS control or phage
460 alone (Figure 6A, B). Whilst injection with heat-killed (HK) SHEF2 phage post-infection with
461 strain OS16 did not improve mortality rates of the zebrafish (73% dead, identical to OS16 only),
462 injection of live SHEF2 resulted in only 16% death (and thus 84% survival) (p<0.0001, vs OS16
463 only). Of note, at fish injected with phage only (SHEF2(LIVE)) or inactivated phage (HK-
464 SHEF2) alone were healthy. Morphology and overall health status of the fish was also
465 monitored, showing that viable phage allowed recovery from OS16 infection while the HK-
466 SHEF2 did not (Figure 6B). We also infected embryos with strain EF3, which is not sensitive to
467 SHEF2 infection (Table 2), but still displayed the ability to cause mortality in embryos by 72 hpi
468 (90%, p<0,0001) compared to PBS, live or killed phage alone injected fish (Fig.6B,C).
469 Significantly, neither viable or heat-killed SHEF2 phage caused an improvement in survival
470 when injected alongside strain EF3 with 81.13 (± 5.46%) and 80.13 (± 1.27%) death
471 respectively. In all experiments, the embryos infected with *E. faecalis*-only displayed a lack of
472 circulation, yolk sac and eye abnormalities, alongside pericardiac oedema and spine curvature
473 (Fig. 6D, shown for OS16). In contrast, the majority of phage-treated zebrafish remained healthy
474 throughout the experiment with health status comparable to phage only and PBS-injected
475 controls (Figure 6B).

476

477 **Discussion**

478 In this paper we report the isolation of 5 lytic phage isolated from wastewater using a
479 range of oral and non-oral *E. faecalis* strains. Surprisingly, we were unable to isolate phage

480 from oral samples against our strains, even though we could visualise phage in concentrated
481 saliva (not shown) even though metagenomic evidence from others that the oral cavity is rich in
482 bacteriophage DNA (56).

483 All the phage described in this study (SHEF2, 4, 5, 6 and 7) belonged to the family
484 *Siphoviridae*, a family of phage previously found to target *E. faecalis*, (16, 19, 57, 58), alongside
485 members of the *Myoviridae* (18, 20, 21).

486 Our isolated phage (SHEF2, 4, 5, 6 and 7) possessed differing host ranges, with SHEF2
487 having the broadest. After genome sequencing we found strong similarity between the genome
488 sequences of SHEF2, 4 and 5 (SHEF2 is 92-94% identical to SHEF4 and 5 respectively) but
489 significant divergence in the putative tail gene locus genes (SHEF2_16, _17, SHEF4_08, _09,
490 and SHEF5_53, _52) with evidence of conserved N-terminal domains but different putative
491 bacterial surface receptor binding domains in the C-terminus of these proteins. Similar
492 observations have been made in various species including *Lactococcus lactis* phage (59, 60)
493 and *Streptococcus thermo lus* phage DT1 where interchange of the C-terminal domain of
494 ORF18 with that of another phage (MD4) altered host-range specificity (61). We suggest that tail
495 module genes four and five encode host-range specificity determining tail proteins that contain
496 potentially novel *E. faecalis* surface binding domains. These findings will open the way for
497 further investigation of phage host specificity and adhesion of Gram-positive bacteria.

498 To probe the cell surface receptor for the SHEF2 phage we showed that it was unable to
499 productively infect insertion mutants with altered core EPA (*epaB*) or EPA decoration genes. All
500 decoration mutants showed reduction in infectivity except for *OPDV_11714::Tn2.14*.. The partial
501 infectivity of *OPDV_11714::Tn2.14* is in line with previous observations showing that mutation of
502 this gene has only a small impact on EPA decoration (22). For both the *epaB* and _11720
503 (decoration) strains the lack of infectivity is despite the phage retaining the ability to adsorb to

the bacterial cell surface. Interestingly there is a discrepancy between the amount of phage recovered from the cell surface of TX5179 and *OPDV_11720::Tn2.5* with more phage still bound to the decoration deficient mutant. This data suggests that SHEF2 likely binds to both the core polysaccharide and decoration residues, and needs both for infection. In a similar manner, this is also the case for several well-characterised bacteriophage, e.g. *E.coli* T4 phage (which requires LPS and OmpC binding) (62) or *S. aureus* phage 3C that requires teichoic and peptidoglycan for irreversible binding (47, 63).

For phages infecting Gram-positive organisms, the injection of viral DNA requires crossing the peptidoglycan layer and interaction with the cell membrane. This process has been studied in *L. lactis* phages that bind to rhamnose moieties of the cell wall before engaging the plasma membrane of the host (64-66). This process often employs phage encoded glycosidases, or lysozyme like enzymes (47), with all the sequenced SHEF phage also encoding a tail protein with putative lyzosyme domain (SHEF2_15, SHEF4_07 and SHEF5_54). Evidence for two-stage adsorption and infection of *E. faecalis* exists in the case of *E. faecalis* and phage VPE25 infection, where a plasma membrane protein (EF0858) seemed to be required for lytic infection (and hence DNA injection) but not phage adsorption to the cell surface receptor (67). We therefore postulate here that the EPA and its variant decoration is required for productive binding of SHEF2 to the cell surface of *E. faecalis* with EPA and an unknown molecule acting as co-receptor for this phage. Based on the evidence in the literature (68, 69) that the Epa PS is not detectable on the outer surface of *E. faecalis* it is tempting to speculate that SHEF2 initially binds first to an outer cell surface PS followed by EPA, but we have no evidence for this. Overall, further tests are required to establish the primary receptor of SHEF2 interaction, potentially by producing recombinant versions of the tail protein domains and investigating their sugar binding properties. Such studies will open new insight into possible

528 resistance mechanisms for phage infection but also new targets for anti-infectives against *E.*
529 *faecalis* or strain specific diagnostics based on cell wall component binding capability.

530 The capacity to form biofilms is critical for *E. faecalis* virulence, providing resistance to
531 antibiotics and allowing infections to persist. Studies have shown a strong association between
532 virulence and biofilm formation with 15-80% of clinical isolates being classified as strong biofilm
533 formers (70-72) In addition, 75% of enterococcal infections in humans (bloodstream, urinary
534 tract, and wound infections) are caused by *E. faecalis* (2). We showed that SHEF2 can
535 significantly reduce biofilm formation of a range of sensitive *E. faecalis* strains (3-10-fold) that
536 were pre-formed (24h) on polystyrene surfaces (mimicking catheters for example) as well as on
537 a novel *in vitro* tooth-cross-section biofilm model (i.e. human tooth cross sections). We believe
538 this to be a strong indication that phage therapy based on SHEF2 and potentially our other
539 phage might be useful for eradication of root-canal infections. In support of our data an *ex-vivo*
540 root canal model, developed by Khalifa et al., 2015, was also significantly cleared of bacteria by
541 phage (20). The use of bacteriophages therefore appears to be a promising strategy to reduce
542 the biofilm bacterial load associated with *E. faecalis* infections, providing a potential adjunctive
543 therapy for root canal infection that has failed to respond to conventional treatment. Other oral
544 infections such as periodontal disease, which is a complex mixed species infection would
545 require phages targeting other oral pathogenic bacteria. However, based on reports of phage
546 targetting *Aggregatibacter actinomycetemcomitans* (73), and *Fusobacterium spp.* (74, 75),
547 alongside several *Streptococcus* (76),, *Veilionella* (77) *and Neisseria spp* (78) in the literature
548 this may be a feasible future approach.

549 In addition to oral infections, *E. faecalis* is a well-known cause of septicaemia (79) with
550 reports showing that oral bacteria can enter the bloodstream and disseminate systemically,
551 contributing to infections such as endocarditis and rheumatoid arthritis (79, 80). We tested the
552 therapeutic potential of the phages we isolated in a well-established *in vivo* zebrafish embryo

553 systemic infection model. We showed, for the first time, that systemic phage treatment after
554 infection with *E. faecalis*, dramatically decreased the mortality of zebrafish embryos and greatly
555 improved their health during infection, indicating the potential of this phage in treating systemic
556 *E. faecalis* infections. It is important to note that neither the phage or bacterial components
557 released upon lysis displayed toxicity toward the embryo further demonstrating potential for safe
558 use of phage systemically. The zebrafish infection model also served extremely well as a
559 system to test the efficacy of phage against systemic bacteria and act as powerful tool for
560 monitoring the dynamics of infection and phage clearance of infection that can be monitored in
561 real-time (81). Given the effectiveness of the phages described in killing planktonic and biofilm
562 associated *E. faecalis,* as well as in a systemic infection model their therapeutic use could be
563 extended to other infection types such as sepsis, wound infections or urinary tract infections.

564 It is well documented that bacteria can gain resistance to bacteriophages, and indeed
565 resistance to *E. faecalis* phage has been previously reported (82). However, we did not isolate
566 resistant strains during our experiments, but cannot rule out that this could occur and consider
567 that the use of a cocktail of phage targeting different cellular receptors would be the best mode
568 to reduce and combat resistance arising. Of note here is that resistance arising to at least
569 phage SHEF2 for example, would require alterations in the EPA core or variable moieties, an
570 alteration that would likely result in reduced virulence (22). It is worth noting here that many of
571 the strains that were sensitive to our small panel of phage in this study were resistant to a range
572 of antibiotics, including vancomycin (e,g, strain V583), and illustrating that phage have the
573 potential to be used as an adjunct or alternative treatment in infections caused by antibiotic
574 resistant strains of important human pathogens.

575 In conclusion, this study highlights isolation of phage targeting *E. faecalis* strains
576 targeting a major virulence determinant of this strain (EPA), and establishes their potential use
577 in treating biofilm infections by testing them in two clinically relevant model infection systems. .

578 Our work thus strenghtens the possibility of developing phage as therapeutics to combat hard-
579 to-treat oral, topical and systemic infections.

580

581 **ACKNOWLEDGMENTS**

582 MA was funded by a scholarship from the Iraqi High commission. We thank Barbara
583 Murray, Gunnar Dahlen and Wim Crielaard for *E. faecalis* strains used in this work. We also
584 thank Chris Hill at the Electron Microscopy unit for assistance and training for the TEM work and
585 MicrobesNG (http://www.microbesng.uk) for sequencing. We also thank Prof. Nic Martin,
586 Sheffield, for help in designing and providing the material for the tooth cross-sectional model.
587 EC was funded by a EPSRC Grand Challenge Twenty65 grant (EP/N010124/1). RES was
588 funded by a Biotechnology and Biological Sciences Research Council studentship
589 (grant BB/M011151/1).

590

591

592

593

594

595 **REFERENCES**:

596

597 1. Wisplinghoff H, Bischoff T, Tallent SM, Seifert H, Wenzel RP, Edmond MB. 2004.
598 Nosocomial bloodstream infections in US hospitals: analysis of 24,179 cases from a
599 prospective nationwide surveillance study. Clinical infectious diseases 39:309-317.
600 2. Gilmore MS, Lebreton F, van Schaik W. 2013. Genomic transition of enterococci from
601 gut commensals to leading causes of multidrug-resistant hospital infection in the
602 antibiotic era. Current opinion in microbiology 16:10-16.
603 3. Paulsen IT, Banerjei L, Myers G, Nelson K, Seshadri R, Read TD, Fouts DE, Eisen JA,
604 Gill SR, Heidelberg J. 2003. Role of mobile DNA in the evolution of vancomycin-resistant
605 *Enterococcus faecalis*. Science 299:2071-2074.
606 4. Polidori M, Nuccorini A, Tascini C, Gemignani G, Iapoce R, Leonildi A, Tagliaferri E,
607 Menichetti F. 2011. Vancomycin-resistant *Enterococcus faecium* (VRE) bacteremia in
608 infective endocarditis successfully treated with combination daptomycin and tigecycline.
609 Journal of chemotherapy (Florence, Italy) 23:240.
610 5. Love R. 2001. *Enterococcus faecalis*–a mechanism for its role in endodontic failure.
611 International endodontic journal 34:399-405.
612 6. Gopikrishna V, Kandaswamy D, Jeyavel RK. 2006. Comparative evaluation of the
613 antimicrobial efficacy of five endodontic root canal sealers against *Enterococcus faecalis*
614 and *Candida albicans*. Journal of Conservative Dentistry 9:2.
615 7. Abdullah M, Ng YL, Gulabivala K, Moles DR, Spratt DA. 2005. Susceptibilties of two
616 *Enterococcus faecalis* phenotypes to root canal medications. J Endod 31:30-6.
617 8. Figdor D, Davies J, Sundqvist G. 2003. Starvation survival, growth and recovery of
618 *Enterococcus faecalis* in human serum. Oral microbiology and immunology 18:234-239.

9. Mohamed JA, Huang W, Nallapareddy SR, Teng F, Murray BE. 2004. Influence of origin of isolates, especially endocarditis isolates, and various genes on biofilm formation by *Enterococcus faecalis*. Infection and immunity 72:3658-3663.

10. Leclercq R. 1997. Enterococci acquire new kinds of resistance. Clinical Infectious Diseases 24:S80-S84.

11. Hunt C. 1998. The emergence of enterococci as a cause of nosocomial infection. British journal of biomedical science 55:149.

12. Rose T, Verbeken G, De Vos D, Merabishvili M, Vaneechoutte M, Lavigne R, Jennes S, Zizi M, Pirnay JP. 2014. Experimental phage therapy of burn wound infection: difficult first steps. International journal of burns and trauma 4:66-73.

13. Rhoads D, Wolcott R, Kuskowski M, Wolcott B, Ward L, Sulakvelidze A. 2009. Bacteriophage therapy of venous leg ulcers in humans: results of a phase I safety trial. Journal of wound care 18.

14. Wright A, Hawkins C, Änggård E, Harper D. 2009. A controlled clinical trial of a therapeutic bacteriophage preparation in chronic otitis due to antibiotic-resistant *Pseudomonas aeruginosa*; a preliminary report of efficacy. Clinical otolaryngology 34:349-357.

15. Dedrick RM, Guerrero-Bustamante CA, Garlena RA, Russell DA, Ford K, Harris K, Gilmour KC, Soothill J, Jacobs-Sera D, Schooley RT, Hatfull GF, Spencer H. 2019. Engineered bacteriophages for treatment of a patient with a disseminated drug-resistant Mycobacterium abscessus. Nat Med 25:730-733.

16. Son J, Jun S, Kim E, Park J, Paik H, Yoon S, Kang S, Choi YJ. 2010. Complete genome sequence of a newly isolated lytic bacteriophage, EFAP-1 of *Enterococcus faecalis*, and antibacterial activity of its endolysin EFAL-1. Journal of applied microbiology 108:1769-1779.

644 17. Fard RMN, Barton MD, Heuzenroeder MW. 2010. Novel bacteriophages in
645 *Enterococcus* spp. Current microbiology 60:400-406.
646 18. Uchiyama J, Rashel M, Maeda Y, Takemura I, Sugihara S, Akechi K, Muraoka A,
647 Wakiguchi H, Matsuzaki S. 2008. Isolation and characterization of a novel *Enterococcus*
648 *faecalis* bacteriophage φEF24C as a therapeutic candidate. FEMS microbiology letters
649 278:200-206.
650 19. Li X, Ding P, Han C, Fan H, Wang Y, Mi Z, Feng F, Tong Y. 2014. Genome analysis of
651 *Enterococcus faecalis* bacteriophage IME-EF3 harboring a putative metallo-beta-
652 lactamase gene. Virus genes 49:145-151.
653 20. Khalifa L, Brosh Y, Gelman D, Coppenhagen-Glazer S, Beyth S, Poradosu-Cohen R,
654 Que Y-A, Beyth N, Hazan R. 2015. Targeting *Enterococcus faecalis* biofilms with phage
655 therapy. Applied and environmental microbiology 81:2696-2705.
656 21. Khalifa L, Coppenhagen-Glazer S, Shlezinger M, Kott-Gutkowski M, Adini O, Beyth N,
657 Hazan R. 2015. Complete genome sequence of *Enterococcus* bacteriophage EFLK1.
658 Genome announcements 3:e01308-15.
659 22. Smith RE, Salamaga B, Szkuta P, Hajdamowicz N, Prajsnar TK, Bulmer GS, Fontaine T,
660 Kolodziejczyk J, Herry JM, Hounslow AM, Williamson MP, Serror P, Mesnage S. 2019.
661 Decoration of the enterococcal polysaccharide antigen EPA is essential for virulence,
662 cell surface charge and interaction with effectors of the innate immune system. PLoS
663 Pathog 15:e1007730.
664 23. Yamamoto KR, Alberts BM, Benzinger R, Lawhorne L, Treiber G. 1970. Rapid
665 bacteriophage sedimentation in the presence of polyethylene glycol and its application to
666 large-scale virus purification. Virology 40:734-744.
667 24. Carlson K, Miller E. 1994. Single-step growth. Molecular biology of bacteriophage 4:434-
668 437.

669 25. Jamet E, Akary E, Poisson MA, Chamba JF, Bertrand X, Serror P. 2012. Prevalence and
670 characterization of antibiotic resistant Enterococcus faecalis in French cheeses. Food
671 Microbiol 31:191-8.
672 26. Ruiz-Garbajosa P, Bonten MJ, Robinson DA, Top J, Nallapareddy SR, Torres C, Coque
673 TM, Canton R, Baquero F, Murray BE, del Campo R, Willems RJ. 2006. Multilocus
674 sequence typing scheme for Enterococcus faecalis reveals hospital-adapted genetic
675 complexes in a background of high rates of recombination. J Clin Microbiol 44:2220-8.
676 27. Feil EJ, Li BC, Aanensen DM, Hanage WP, Spratt BG. 2004. eBURST: inferring patterns
677 of evolutionary descent among clusters of related bacterial genotypes from multilocus
678 sequence typing data. J Bacteriol 186:1518-30.
679 28. Wood DE, Salzberg SL. 2014. Kraken: ultrafast metagenomic sequence classification
680 using exact alignments. Genome biology 15:R46.
681 29. Li H. 2013. Aligning sequence reads, clone sequences and assembly contigs with BWA-
682 MEM. arXiv preprint arXiv:13033997.
683 30. Bolger AM, Lohse M, Usadel B. 2014. Trimmomatic: a flexible trimmer for Illumina
684 sequence data. Bioinformatics:btu170.
685 31. Bankevich A, Nurk S, Antipov D, Gurevich AA, Dvorkin M, Kulikov AS, Lesin VM,
686 Nikolenko SI, Pham S, Prjibelski AD. 2012. SPAdes: a new genome assembly algorithm
687 and its applications to single-cell sequencing. Journal of computational biology 19:455-
688 477.
689 32. Seemann T. 2014. Prokka: rapid prokaryotic genome annotation. Bioinformatics:btu153.
690 33. Darling AC, Mau B, Blattner FR, Perna NT. 2004. Mauve: multiple alignment of
691 conserved genomic sequence with rearrangements. Genome research 14:1394-1403.
692 34. Corpet F. 1988. Multiple sequence alignment with hierarchical clustering. Nucleic acids
693 research 16:10881-10890.

694 35. Zhou Y, Liang Y, Lynch KH, Dennis JJ, Wishart DS. 2011. PHAST: a fast phage search
695 tool. Nucleic acids research:gkr485.
696 36. Arndt D, Grant JR, Marcu A, Sajed T, Pon A, Liang Y, Wishart DS. 2016. PHASTER: a
697 better, faster version of the PHAST phage search tool. Nucleic acids research 44:W16-
698 W21.
699 37. Sonnhammer EL, Eddy SR, Durbin R. 1997. Pfam: a comprehensive database of protein
700 domain families based on seed alignments. Proteins-Structure Function and Genetics
701 28:405-420.
702 38. Rutherford K, Parkhill J, Crook J, Horsnell T, Rice P, Rajandream M-A, Barrell B. 2000.
703 Artemis: sequence visualization and annotation. Bioinformatics 16:944-945.
704 39. O'Toole GA, Kolter R. 1998. Initiation of biofilm formation in *Pseudomonas fluorescens*
705 WCS365 proceeds via multiple, convergent signalling pathways: a genetic analysis. Mol
706 Microbiol 28:449-61.
707 40. Yoon H, Yun J, Lim J-A, Roh E, Jung K-S, Chang Y, Ryu S, Heu S. 2013.
708 Characterization and genomic analysis of two *Staphylococcus aureus* bacteriophages
709 isolated from poultry/livestock farms. Journal of General Virology 94:2569-2576.
710 41. O'brien J, Wilson I, Orton T, Pognan F. 2000. Investigation of the Alamar Blue
711 (resazurin) fluorescent dye for the assessment of mammalian cell cytotoxicity. European
712 Journal of Biochemistry 267:5421-5426.
713 42. Perrot S, Dutertre-Catella H, Martin C, Rat P, Warnet J-M. 2003. Resazurin metabolism
714 assay is a new sensitive alternative test in isolated pig cornea. Toxicological sciences
715 72:122-129.
716 43. Widziolek M, Prajsnar TK, Tazzyman S, Stafford GP, Potempa J, Murdoch C. 2016.
717 Zebrafish as a new model to study effects of periodontal pathogens on cardiovascular
718 diseases. Scientific reports 6:36023.

719 44. Ackermann H-W. 2007. 5500 Phages examined in the electron microscope. Archives of
720 virology 152:227-243.
721 45. Fujisawa H, Morita M. 1997. Phage DNA packaging. Genes to Cells 2:537-545.
722 46. Sun S, Gao S, Kondabagil K, Xiang Y, Rossmann MG, Rao VB. 2012. Structure and
723 function of the small terminase component of the DNA packaging machine in T4-like
724 bacteriophages. Proceedings of the National Academy of Sciences 109:817-822.
725 47. Rakhuba D, Kolomiets E, Dey ES, Novik G. 2010. Bacteriophage receptors,
726 mechanisms of phage adsorption and penetration into host cell. Pol J Microbiol 59:145-
727 155.
728 48. Chapot-Chartier M-P. 2014. Interactions of the cell-wall glycopolymers of lactic acid
729 bacteria with their bacteriophages. Frontiers in microbiology 5:236.
730 49. Xu Y, Murray BE, Weinstock GM. 1998. A cluster of genes involved in polysaccharide
731 biosynthesis from *Enterococcus faecalis* OG1RF. Infection and immunity 66:4313-4323.
732 50. Hancock LE, Shepard BD, Gilmore MS. 2003. Molecular analysis of the *Enterococcus*
733 *faecalis* serotype 2 polysaccharide determinant. Journal of bacteriology 185:4393-4401.
734 51. Teng F, Singh KV, Bourgogne A, Zeng J, Murray BE. 2009. Further characterization of
735 the *epa* gene cluster and Epa polysaccharides of *Enterococcus faecalis*. Infection and
736 immunity 77:3759-3767.
737 52. Rigottier-Gois L, Madec C, Navickas A, Matos RC, Akary-Lepage E, Mistou MY, Serror
738 P. 2015. The surface rhamnopolysaccharide epa of Enterococcus faecalis is a key
739 determinant of intestinal colonization. J Infect Dis 211:62-71.
740 53. Hall-Stoodley L, Costerton JW, Stoodley P. 2004. Bacterial biofilms: from the natural
741 environment to infectious diseases. Nature reviews microbiology 2:95-108.
742 54. Høiby N, Ciofu O, Johansen HK, Song Z-j, Moser C, Jensen PØ, Molin S, Givskov M,
743 Tolker-Nielsen T, Bjarnsholt T. 2011. The clinical impact of bacterial biofilms.
744 International journal of oral science 3:55.

745 55. Prajsnar TK, Renshaw SA, Ogryzko NV, Foster SJ, Serror P, Mesnage S. 2013.
746 Zebrafish as a novel vertebrate model to dissect enterococcal pathogenesis. Infection
747 and immunity 81:4271-4279.
748 56. Ly M, Abeles SR, Boehm TK, Robles-Sikisaka R, Naidu M, Santiago-Rodriguez T, Pride
749 DT. 2014. Altered oral viral ecology in association with periodontal disease. MBio
750 5:e01133-14.
751 57. Fard RMN, Barton MD, Arthur JL, Heuzenroeder MW. 2010. Whole-genome sequencing
752 and gene mapping of a newly isolated lytic enterococcal bacteriophage EFRM31.
753 Archives of virology 155:1887-1891.
754 58. Zhang W, Mi Z, Yin X, Fan H, An X, Zhang Z, Chen J, Tong Y. 2013. Characterization of
755 Enterococcus faecalis phage IME-EF1 and its endolysin. PLoS One 8:e80435.
756 59. Stuer-Lauridsen B, Janzen T, Schnabl J, Johansen E. 2003. Identification of the host
757 determinant of two prolate-headed phages infecting *Lactococcus lactis*. Virology 309:10-
758 17.
759 60. Lubbers MW, Waterfield NR, Beresford T, Le Page R, Jarvis AW. 1995. Sequencing and
760 analysis of the prolate-headed lactococcal bacteriophage c2 genome and identification
761 of the structural genes. Applied and environmental microbiology 61:4348-4356.
762 61. Duplessis M, Moineau S. 2001. Identification of a genetic determinant responsible for
763 host specificity in *Streptococcus thermophilus* bacteriophages. Molecular microbiology
764 41:325-336.
765 62. Yu F, Mizushima S. 1982. Roles of lipopolysaccharide and outer membrane protein
766 OmpC of Escherichia coli K-12 in the receptor function for bacteriophage T4. Journal of
767 bacteriology 151:718-722.
768 63. Coyette J, Ghuysen JM. 1968. Structure of the cell wall of *Staphylococcus aureus*. IX.
769 Teichoic acid and phage adsorption. Biochemistry 7:2385-2389.

64. Geller BL, Ivey RG, Trempy JE, Hettinger-Smith B. 1993. Cloning of a chromosomal gene required for phage infection of *Lactococcus lactis* subsp. *lactis* C2. Journal of bacteriology 175:5510-5519.

65. Monteville MR, Ardestani B, Geller BL. 1994. *Lactococcal* bacteriophages require a host cell wall carbohydrate and a plasma membrane protein for adsorption and ejection of DNA. Applied and environmental microbiology 60:3204-3211.

66. Babu K, Spence W, Monteville M, Geller B. 1994. Characterization of a cloned gene (pip) from *lactococcus lactis* required for phage infection. Developments in biological standardization 85:569-575.

67. Duerkop BA, Huo W, Bhardwaj P, Palmer KL, Hooper LV. 2016. Molecular basis for lytic bacteriophage resistance in enterococci. MBio 7:e01304-16.

68. Xu Y, Singh KV, Qin X, Murray BE, Weinstock GM. 2000. Analysis of a gene cluster of *Enterococcus faecalis* involved in polysaccharide biosynthesis. Infection and immunity 68:815-823.

69. Hancock LE, Gilmore MS. 2002. The capsular polysaccharide of *Enterococcus faecalis* and its relationship to other polysaccharides in the cell wall. Proceedings of the National Academy of Sciences 99:1574-1579.

70. Baldassarri L, Cecchini R, Bertuccini L, Ammendolia MG, Iosi F, Arciola CR, Montanaro L, Di Rosa R, Gherardi G, Dicuonzo G. 2001. *Enterococcus* spp. produces slime and survives in rat peritoneal macrophages. Medical microbiology and immunology 190:113-120.

71. Di Rosa R, Creti R, Venditti M, D'Amelio R, Arciola CR, Montanaro L, Baldassarri L. 2006. Relationship between biofilm formation, the enterococcal surface protein (Esp) and gelatinase in clinical isolates of *Enterococcus faecalis* and *Enterococcus faecium*. FEMS microbiology letters 256:145-150.

72. Toledo-Arana A, Valle J, Solano C, Arrizubieta MaJ, Cucarella C, Lamata M, Amorena B, Leiva J, Penadés JR, Lasa I. 2001. The enterococcal surface protein, Esp, is involved in *Enterococcus faecalis* biofilm formation. Applied and environmental microbiology 67:4538-4545.

73. Castillo-Ruiz M, Vinés ED, Montt C, Fernández J, Delgado JM, Hormazábal JC, Bittner M. 2011. Isolation of a novel *Aggregatibacter actinomycetemcomitans* serotype b bacteriophage capable of lysing bacteria within a biofilm. Applied and environmental microbiology 77:3157-3159.

74. Machuca P, Daille L, Vinés E, Berrocal L, Bittner M. 2010. Isolation of a novel bacteriophage specific for the periodontal pathogen *Fusobacterium nucleatum*. Applied and environmental microbiology 76:7243-7250.

75. Szafrański SP, Winkel A, Stiesch M. 2017. The use of bacteriophages to biocontrol oral biofilms. Journal of biotechnology 250:29-44.

76. Dalmasso M, De Haas E, Neve H, Strain R, Cousin FJ, Stockdale SR, Ross RP, Hill C. 2015. Isolation of a novel phage with activity against *Streptococcus mutans* biofilms. PloS one 10:e0138651.

77. Hiroki H, Shiiki J, Handa A, Totsuka M, Nakamura O. 1976. Isolation of bacteriophages specific for the genus *Veillonella*. Archives of oral biology 21:215-217.

78. Aljarbou AN, Aljofan M. 2014. Genotyping, morphology and molecular characteristics of a lytic phage of *Neisseria* strain obtained from infected human dental plaque. Journal of Microbiology 52:609-618.

79. Li X, Kolltveit KM, Tronstad L, Olsen I. 2000. Systemic diseases caused by oral infection. Clinical microbiology reviews 13:547-558.

80. Scher JU, Abramson SB. 2011. The microbiome and rheumatoid arthritis. Nature Reviews Rheumatology 7:569-578.

81. Qazi S, Harrison S, Self T, Williams P, Hill P. 2004. Real-time monitoring of intracellular *Staphylococcus aureus* replication. Journal of bacteriology 186:1065-1077.

82. Khalifa L, Gelman D, Shlezinger M, Dessal AL, Coppenhagen-Glazer S, Beyth N, Hazan R. 2018. Defeating Antibiotic- and Phage-Resistant Enterococcus faecalis Using a Phage Cocktail in Vitro and in a Clot Model. Front Microbiol 9:326.

83. Sedgley C, Lennan S, Clewell D. 2004. Prevalence, phenotype and genotype of oral enterococci. Oral microbiology and immunology 19:95-101.

84. Sedgley C, Nagel A, Shelburne C, Clewell D, Appelbe O, Molander A. 2005. Quantitative real-time PCR detection of oral *Enterococcus faecalis* in humans. Archives of oral biology 50:575-583.

85. Johnson EM, Flannagan SE, Sedgley CM. 2006. Coaggregation Interactions Between Oral and Endodontic *Enterococcus faecalis* and Bacterial Species Isolated From Persistent Apical Periodontitis. Journal of endodontics 32:946-950.

86. Dahlen G, Blomqvist S, Almståhl A, Carlen A. 2012. Virulence factors and antibiotic susceptibility in enterococci isolated from oral mucosal and deep infections. Journal of oral microbiology 4.

87. Bourgogne A, Garsin DA, Qin X, Singh KV, Sillanpaa J, Yerrapragada S, Ding Y, Dugan-Rocha S, Buhay C, Shen H. 2008. Large scale variation in *Enterococcus faecalis* illustrated by the genome analysis of strain OG1RF. Genome biology 9:R110.

88. Zeng J, Teng F, Weinstock GM, Murray BE. 2004. Translocation of Enterococcus faecalis strains across a monolayer of polarized human enterocyte-like T84 cells. J Clin Microbiol 42:1149-54.

89. Jacob AE, Hobbs SJ. 1974. Conjugal transfer of plasmid-borne multiple antibiotic resistance in *Streptococcus faecalis* var. *zymogenes*. Journal of Bacteriology 117:360-372.

90. Van den Bogaard A, Mertens P, London N, Stobberingh E. 1997. High prevalence of colonization with vancomycin-and pristinamycin-resistant enterococci in healthy humans and pigs in The Netherlands: is the addition of antibiotics to animal feeds to blame? Journal of Antimicrobial Chemotherapy 40:454-456.

874 **TABLES**

875 **Table 1. Bacterial strains used in the study.**

Bacterial strain	Source	Reference
E. faecalis		
EF1,EF2,EF3 OS16	Oral rinse-endodontic patient	(83) (84)
ER3/2s	Oral orthograde retreatment	(85)
OMGS3197, OMGS3198	Oral endodontic strains	(86)
OMGS3885, OMGS3919	Oral mucosal lesions	(86)
EF54	Non oral human isolate	(72)
OG1RF	Oral lab strain	(87)
OG1RF *epaB* TX5179; mutant harbouring an insertion in *epaB* (formerly *orfde4*)		(68)
OG1RF *epaB* TX5179 +pTX5249	Complementation plasmid build and strain constructed by Zeng et al (2004)	(88)
OG1RF OPDV; OG1RF derivative with deletions in *oatA*, *pgdA*, *dltA* and *sigV*	Constructed by Smith et al (2019)	(22)
OPDV_11720::Tn2.5; A transposon mutant harbouring a mutation in *OG1RF_11720*	Isolated by Smith et al (22)	(22)
OPDV_11720::Tn2.5 + pTet-*OG1RF_11720*	Complementation plasmid built and strain constructed by Smith et al (22)	(22)
OPDV_11715::Tn2.13; A transposon mutant harbouring a mutation in *OG1RF_11715*	Isolated by Smith et al (22)	(22)
OPDV_11715::Tn2.13 + pTet-*OG1RF_11715*	Complementation plasmid build and strain constructed by Smith et al (22)	(22)
OPDV_11714::Tn2.14; A transposon mutant harbouring a mutation in *OG1RF_11714*	Isolated by Smith et al (22)	(22)

OPDV_11714::Tn2.14 + pTet-*OG1RF_11714*	Complementation plasmid build and strain constructed by Smith et al (2019)	(22)
OPDV_11707::Tn2.8; A transposon mutant harbouring a mutation in *OG1RF_11714*	Isolated by Smith et al (2019)	(22)
OPDV_11707::Tn2.8 + pTet-*OG1RF_11707*	Complementation plasmid build and strain constructed by Smith et al (2019)	(22)
JH2-2	Non oral lab strain	(89)
E. faecium E1162	Clinical blood isolate; CC17	(90)

Table 2. Head and tail dimensions of isolated *E. faecalis* phages. At least three phage particles were measured for each phage type and the mean value used for calculating dimensions.

Phage	Head diameter (nm)	Tail length (nm)
SHEF2	42.34 ± 1.0	231 ± 1.3
SHEF4	45.60 ± 1.0	199.4 ± 0.8
SHEF5	44.32 ±0.9	240.5 ± 1.5
SHEF6	45.81 ± 0.4	250.6 ± 3.0
SHEF7	41 ± 0.1	230 ± 2.4

Table 3. Phage-host range of SHEF phages. (+) indicates a zone of clearance in both spot and SAO screening tests and (-) no evidence of clearance. The final column indicates MLST designation established by sequencing according to http://efaecalis.mlst.net/

887

Strain/Phage	SHEF2	SHEF4	SHEF5	SHEF6	SHEF7	MLST
OS16	+	-	+	+	+	173
ER3/2s	+	-	-	+	+	21
EF1	-	-	+	-	-	34
EF2	-	+	-	-	-	283
EF3	-	+	-	-	-	97
EF54	+	-	-	+	+	381
OMGS 3197	+	-	-	+	-	21
OMGS 3198	+	-	-	-	-	55
OMGS 3885	+	-	-	+	-	72
OMGS 3919	+	-	-	+	+	97
OG1RF	+	-	-	+	+	1
V583	+	-	+	-	-	6
JH2-2	-	-	+	-	-	8
Total	**9**	**2**	**4**	**7**	**5**	

888

889

890

891

892

893

894

895

896

897

898

899 **Figure Legends**

Figure 1A. Isolation of *E. faecalis* bacteriophage and plaque morphology. Images of bacterial plaques formed by the isolated phage in top-agar lawns of *E. faecalis* OS16 (SHEF2), *E. faecalis* EF3 (SHEF4), *E. faecalis* EF2 (SHEF5) and *E. faecalis* OMGS3919 (SHEF6 and 7). SHEF7 is also shown with *E. faecalis* OG1RF to illustrate plaque morphologies.

1B. Transmission electron micrographs of SHEF phage particles. Phage were negatively stained with 0.2 % uranyl acetate as described in methods section. Scale bars (100 nm).

1C. Restriction fragment length polymorphism (RFLP) analysis of extracted phage chromosomal DNA SHEF2, 4, 5, , and 7 phages genomic DNA was digested with *Hind*III and analysed by Agarose gel electrophoresis (inverted image shown alongside GeneRuler 1kb ladder).

1D. Virion protein profiles of SHEF 2, 4, 5, 6, and 7 by SDS-PAGE with InsatntBlue staining. The dominant protein band identified my MS/MS as the major capsid protein for SHEF2 at 36 KDa is indicated (*).

Figure 2. Genome organisation of *E. faecalis* lytic phages SHEF2, SHEF5, and SHEF4

2A. Images produced using SnapGene® Viewer 1.1.3 Software (DUF- conserved domains of unknown function). Genome annotation corresponds to GenBank Accession numbers: MF678788, MF678789, and MF678790 for SHEF2, 4 and 5 respectively; with colours corresponding to predicted function as indicated in key.

2B. Mauve alignment of tail and lysis genes highlighting areas of conservation.

Figure 3. Molecular determination of SHEF2 phage adhesion using strain OG1RF.

3A. Schematic of the OG1RF *epa* core (purple) and variable locus (blue). Generated using Snapgene (labelling according to Accession number NC_017316.1).

3B. Table showing qualitative results of spot-assay double layer agar infections of strains listed with SHEF2 (+:infection; -: no infection) (for pictures see Fig S4).

3C. Phage adsorbtion assay for OG1RF and its isogenic mutant strains *epaB* and OPDV_11720 (all at 10^8 CFU/ml bacteria) with SHEF2. Phage (input: $2x10^6$) were added for 24h before phage were enumerated in cell supernatants before and after treatment with 0.28 M NaCl by titre assay. ND-Not Determined (due to all cells being dead). This experiment was repeated twice in triplicate each time (mean shown), with one example displayed here.

3D. TEMs of infected OG1RF, *epaB* and _11720 mutants with SHEF2 at 30 mins post-infection- arrows indicate adsorbed phage.

Figure 4. One step growth and adsorption rate characterisation of SHEF2.

4A. One-step growth curve of SHEF2 phage with *E. faecalis* OS16 as host. The two sets of data represent samples treated with and without chloroform. Eclipse, burst and latent period are labelled.

4B. Adsorption of SHEF2 phage to *E. faecalis* OS16 expressed as a % of total phage added.

4C. Transmission electron micrograph of strain OS16 + SHEF2 at 30 min post infection. black arrows: spent heads and adsorbed phage; white arrow- un adsorbed phage.

Figure 5. Biofilm assay on polystyrene plates and tooth root slices.

5A. Bar charts represent biofilm growth as measured by Crystal violet staining (measured using A570 of extracted stain, normalised to cell growth in each well, A600). Samples treated with live phage are labelled: +SHEF2; while those with heat-killed: +SHEF2 (HK); strain names are as elsewhere. Mean of 6 polystyrene microtitre wells per condition are shown with SD and students t-test to compare conditions ($P<0.0001$). Experiments were conducted on three separate occasions, one example shown.

5B. upper: photograph of tooth root slices in-situ treated with SHEF2 (+SHEF2) or strain EF54 only. The difference in colour represents resazurin reduction to resorufin, and is represented quantitatively below (mean, SD from 3 readings), with Student's t-test was used to compare between treated and untreated groups ($p<0.0001$).

5C. Stereo microscope (ST-left) and light microscope (LM-right, resazurin stained), images represent the untreated group (upper) while the lower images SHEF2 –treated. Biofilm of *E. faecalis* colonies scattered on the root canal surface (RC) and dentinal surface (DS) of the ST and LM images are shown, respectively.

Figure 6. Phage SHEF2 treatment of *E. faecalis* OS16-infected zebrafish embryos. Zebrafish were infected systematically with *E. faecalis* OS16 strain or strain EF3 at a dose of 30,000 CFU at 30 hpf. After 2 hours embryos were injected with SHEF2 (SHEF2 LIVE) phage or heat-inactivated (SHEF2(HK)) at an MOI 20 (in 2nl). Controls were also performed with phage only (SHEF2 LIVE or SHEF2(HK)) and PBS (2nl). Data are presented as Kaplan-Meier survival plots (A,C) as well as bar-chart indicating mortality data at 72hpi or all conditons; Bars represent means ± SD. Three independent experiments were performed (n=20 zebrafish per condition per experiment). Statistical comparison between groups was performed using a log-rank test (A,C) or One-way Anova (B). (6D) Morphology of zebrafish embryos at 72hpi are shown injected with PBS, *E. faecalis* OS16 alone, SHEF2 LIVE alone or *E. faecalis* OS16

967 followed by SHEF2 LIVE (D). Red arrows indicate symptoms of infection (eye and yolk sac
968 abnormalities, spinal curving and pericardial oedema). Scale bar = 500 μm.

969

970

971

972

973

Figure 1

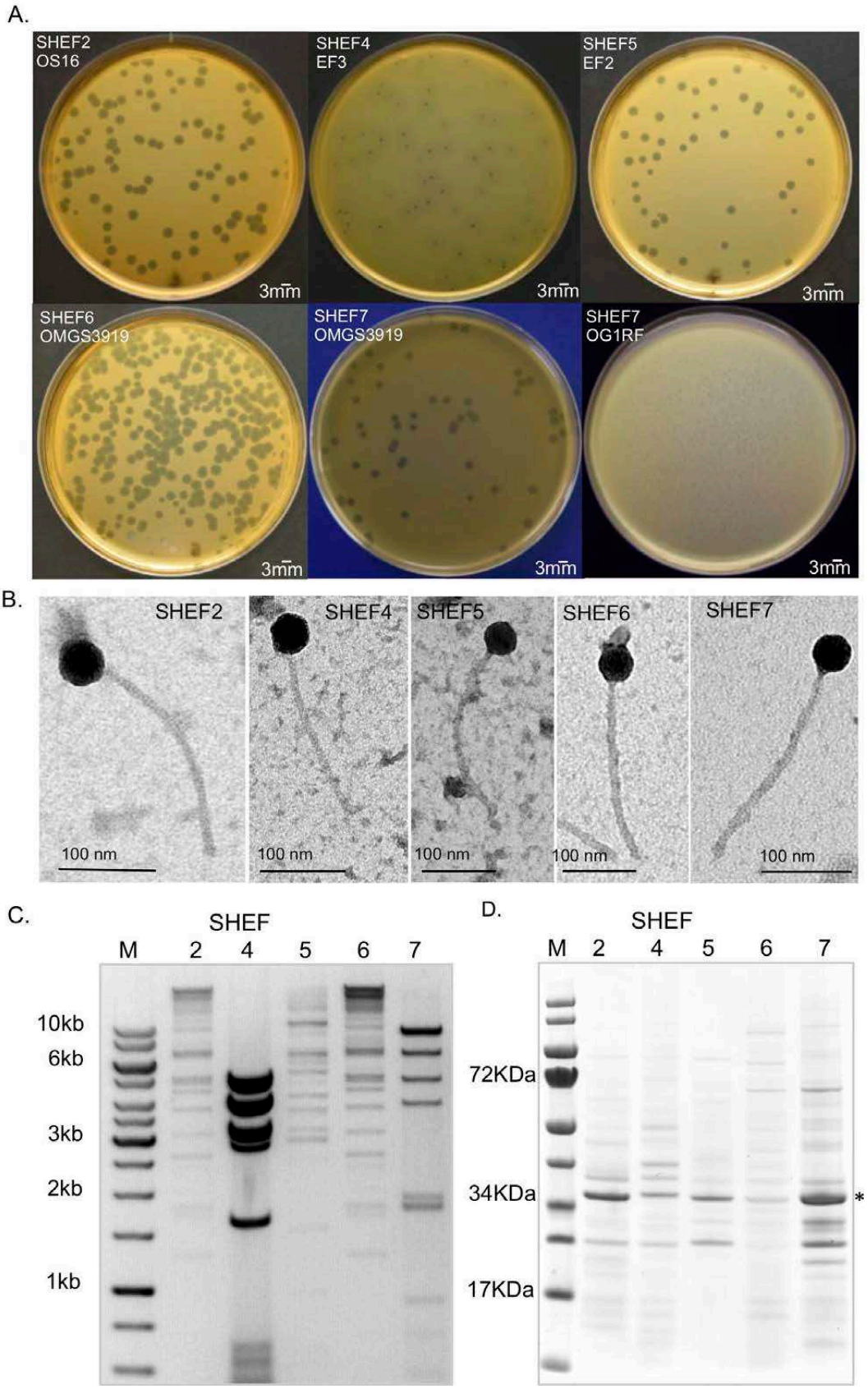

Figure 2

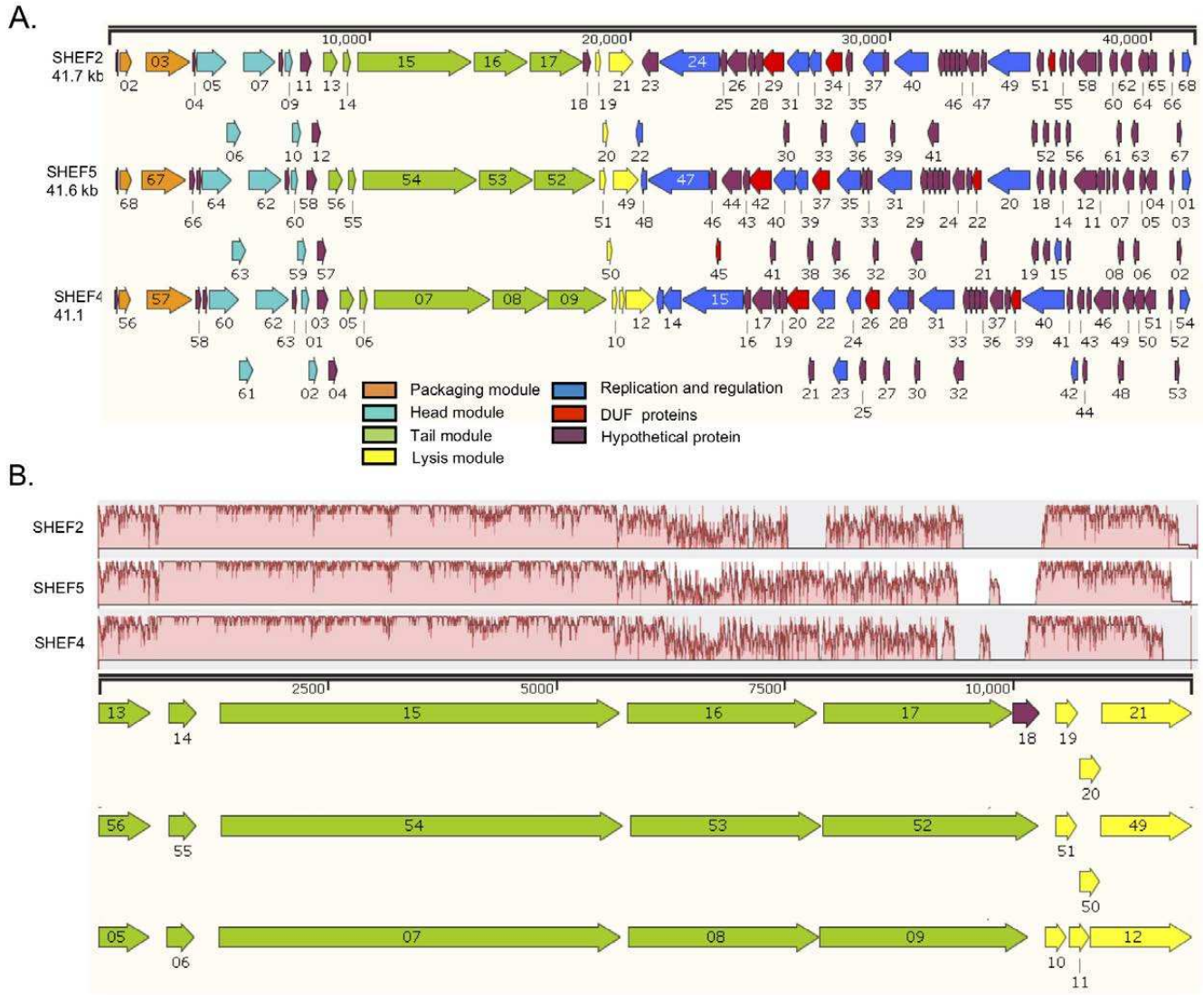

Figure 3

A.

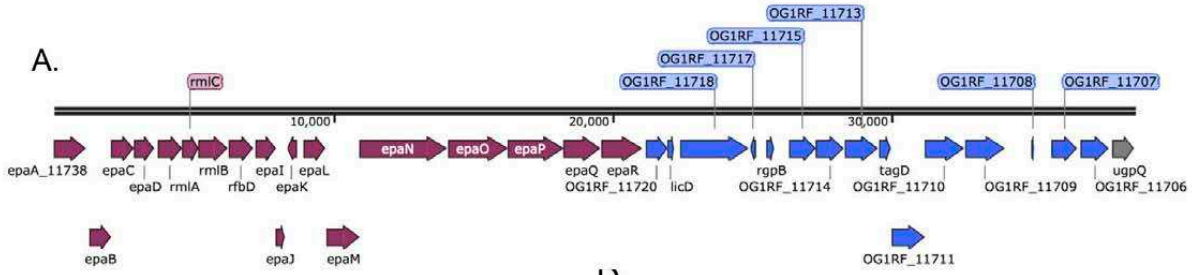

B.

Strain	Phage: SHEF2
OG1RF	+
OG1RF *epaB*	-
OG1RF *epaB_c*	+
OG1RF_OPDV	+
OPDV_11720	-
OPDV_11720_c	+
OPDV_11715	-
OPDV_11715_c	+
OPDV_11714	-
OPDV_11714_c	+
OPDV_11707	-
OPDV_11707_c	+

C.

PFU/ml	OG1RF	*epaB*	OPDV _11720
Input	$2x10^6$	$2x10^6$	$2x10^6$
After 24h	$1x10^{11}$	$2.7x10^5$	$4x10^4$
0.28M NaCl	ND	$1.4x10^5$	700

D.

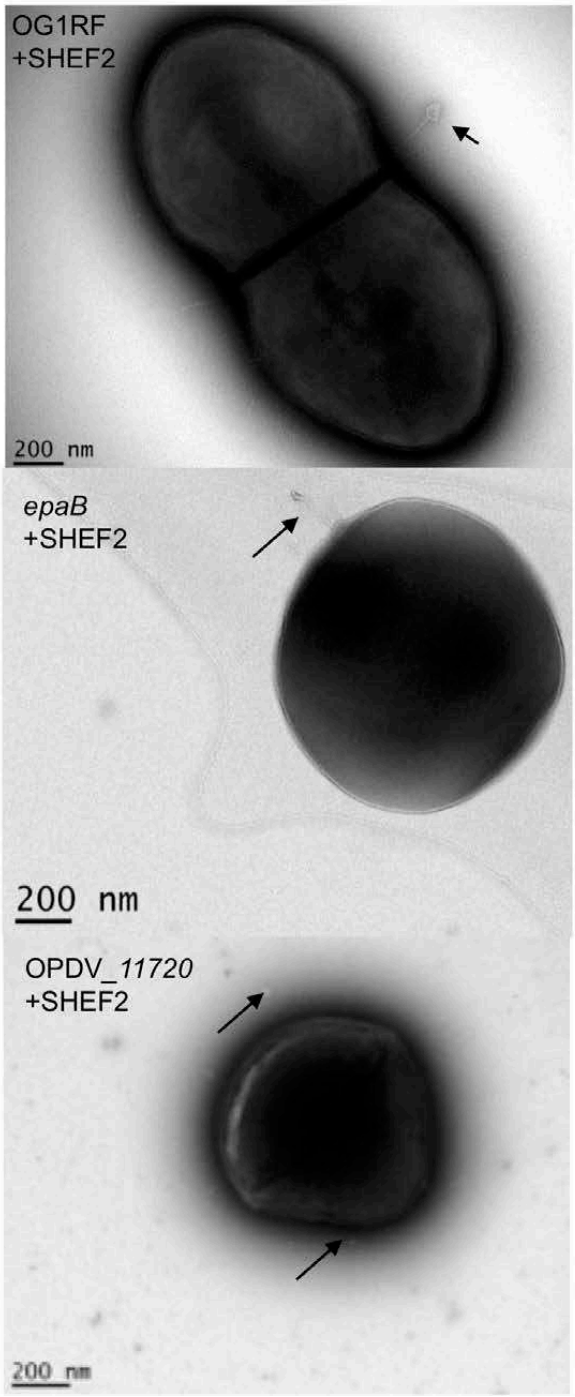

Figure 4

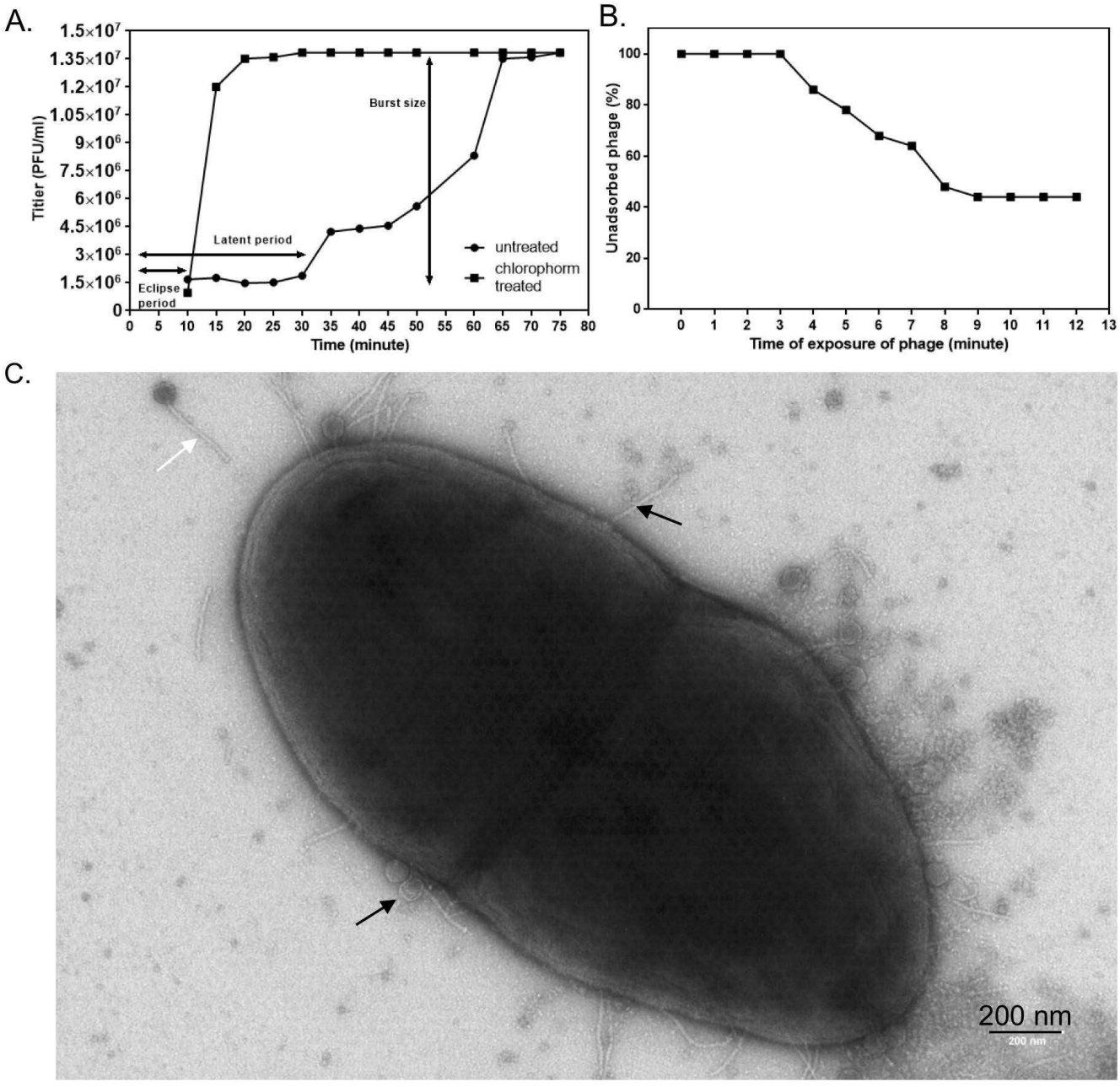

Figure 5

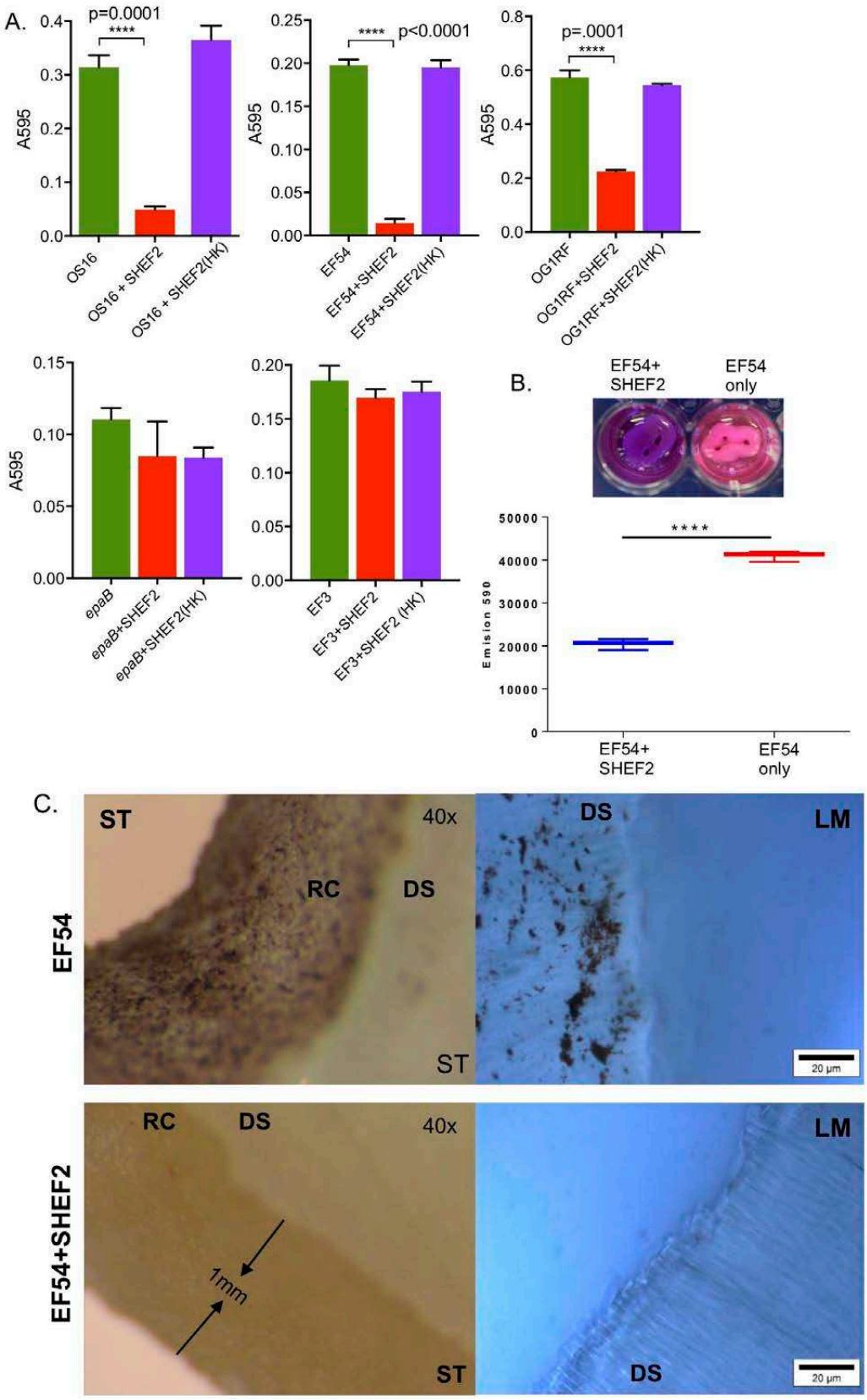

Figure 6